Enhanced Detection of Benzo[a]pyrene in Olive Oil through Low Temperature Liquid-Liquid Extraction Coupled with Constant Energy Synchronous Fluorescence Spectroscopy

Willian M. Soares, [a] **Ricardo M. Orlando** *,[a] **and Helvécio C. Menezes** [b]

[a]*Laboratório de Microfluídica e Separações (LaMS), Departamento de Química, Universidade Federal de Minas Gerais (UFMG), Av. Pres. Antônio Carlos, 6627, 31270-901 Belo Horizonte-MG, Brazil*

[b]*Rede Mineira de Cromatografia Avançada (RMCA), Departamento de Química, Universidade Federal de Minas Gerais (UFMG), Av. Pres. Antônio Carlos, 6627, 31270-901 Belo Horizonte-MG, Brazil*

Refined processed olive oil can indeed become significantly contaminated with polycyclic aromatic hydrocarbons (PAHs). To assess exposure to these contaminants, benzo[a]pyrene (B[a]P) is utilized as a marker due to its known carcinogenicity in humans. The European Commission has established a maximum limit of 2 µg kg^{-1} for B[a]P in edible oils. However, the analysis of trace amounts of B[a]P in a complex matrix like olive oil poses a persistent challenge. In this study, we have developed a low-temperature liquid-liquid extraction method in combination with constant energy synchronous fluorescence analysis for the determination of B[a]P in olive oil samples. The analyte was extracted from the olive oil using a mixture of acetonitrile and acetone. The performance of fluorescence measurements was evaluated by carefully considering the effects of solvent, temperature, acetone quenching, and slit width for monochromators. The proposed method demonstrates a linear range from 0.8 to 3.2 µg kg^{-1}, with limits of detection and quantification of 0.04 and 0.80 µg kg^{-1}, respectively. Precision and trueness assessments revealed relative standard deviations of less than 10% and recovery rates ranging from 103 to 112%. This method presents an efficient and rapid alternative to sample preparation procedure that minimizes organic solvent consumption.

Keywords: benzo[a]pyrene, olive oil, fluorescence spectroscopy

Introduction

Polycyclic aromatic hydrocarbons (PAHs) are organic toxic compounds that belong to the group of persistent organic pollutants. These molecules, characterized by the condensation of two or more aromatic rings, are mainly produced during the incomplete combustion of organic matter. They are widely found in the ecosystems and occur by natural events and anthropogenic activities.[1] PAHs are one of the most important health concerns and the subject of extensive research, considering the risks they represent to human health. The Environmental Protection Agency (EPA) established 16 compounds as priority contaminants according to their potential for inducing cancer.[2] Among these substances, benzo[a]pyrene (B[a]P) is the only one included in Class 1 of the International Agency for Research on Cancer (IARC), as it is carcinogenic for humans.[3] Therefore, B[a]P is the most assessed PAH, being used as the main marker for the presence of these contaminants in foods. This PAH is one of the most powerful carcinogenic agents, also exhibiting embryotoxic, mutagenic, and teratogenic effects with evidence of neoplasia observed in fish and mammals only 6 h after they were exposed to 250 µg kg^{-1} of B[a]P.[4-7]

Breathing air or eating contaminated foods is the main form of human exposure to PAHs.[8,9] Vegetable oils are a very regular source of B[a]P in foods due to the lipophilic nature of hydrocarbons and the worldwide consumption.[10] In this context, olive oil has been manifesting alarming levels of PAHs, generally at higher concentration levels than refined vegetable oils because the refinement processes reduce the

*e-mail: orlandoricardo@ufmg.br
Editor handled this article: Eduardo Carasek

contamination considerably.[11,12] Certain conditions enable the insertion of B[*a*]P in olive oils such as the diffusion of polluted air in industrial areas. This substance has high chemical stability and is adsorbed in solid nanoparticles that contact the olives directly or through rain, propagating it to the final product.[13] To reduce the risks associated with oil consumption, the European Commission defines a maximum limit of 2 µg kg^{-1} of B[*a*]P in edible oils.[14]

Oils are complex matrixes like most foods, and as such, their composition has many interferences that make it difficult to determine analytes in trace concentrations. Vegetable oils are composed primarily of triacylglycerols and other glycerol in addition to small amounts of other components (e.g., phospholipids, free sterols, tocopherols, triterpene alcohols, hydrocarbons, and fat-soluble vitamins).[15]

Removing these non-volatile compounds efficiently to preconcentrate and quantify B[*a*]P is not a trivial and easy task because most of the organic solvents used for conventional liquid-liquid extraction lack sufficient selectivity to extract this PAH.[16]

PAHs absorb light in the range of 200-400 nm and are the compounds with the highest natural fluorescence quantum yield. By that means, fluorescence is a compatible analytical technique, being highly selective, sensitive, and extensively used for PAH determination within the range of 0.1 to 1.0 µg L^1.[17] The direct quantification of B[*a*]P by fluorescence can be carried out as a PAH contamination marker, which dismisses the use of chromatography and reduces the analysis time and solvent consumption.[18-25]

Conventional spectrofluorimetry has limitations for crude olive oil characterization because the various substances contained in it may cause auto absorption and signal overlap. These problems can potentially be avoided by using constant energy synchronous fluorescence (CESF). In this configuration, both monochromators vary their respective wavelength values simultaneously during the scanning. However, a fixed Δλ in nm is maintained, which represents the difference between the emission and excitation. It is convenient that the selected Δλ corresponds to the Stokes shift of the fluorophore so that the provided spectrum exclusively evidences the electronic transitions that occur in this energy.[26]

A standardized method for determining PAHs in oils is provided by ISO 15753.[27] This procedure involves the extraction and purification of hydrocarbons using C18 reversed-phase and florisil-bonded-phase cartridges, followed by analysis using high-performance liquid chromatography (HPLC) with a fluorescence detector.[27]

Low temperature liquid-liquid extraction (LTLLE) is an easy cleanup technique and is effective for eliminating fat interferences from oil samples.[28] The extraction is based on the addition of organic solvents and subsequent freezing of the solution at −25 °C or below. After the fat is frozen out, the organic solvent can be simply separated and purified with an alumina-N cartridge.[29] The current state-of-the-art for the quantification of B[*a*]P in olive oil is 0.1 µg kg^{-1} when employing HPLC coupled with a fluorescence detector and 0.3 µg kg^{-1} when utilizing gas chromatography coupled with a mass spectrometer.[30]

The aim of our research was to propose a new, easy, fast, and reliable method for determining B[*a*]P in olive oil. The improvements consisted of executing liquid-liquid extraction just once, replacing the solid phase extraction cleanup by a liquid-liquid extraction carried out at a low temperature, and running the instrumental analysis directly on a fluorescence spectrophotometer. After optimization and figures of merit, some parameters of the developed method such as analysis time, required equipment, and solvent consumption were compared to the reference methods.

Experimental

Chemicals

Analytical grade B[*a*]P (purity ≥ 97%) was purchased from Sigma-Aldrich (St. Louis, MO, USA). Acetonitrile was purchased from Merck (Darmstadt, Germany). Acetone, hexane, ethyl octanoate, and toluene were obtained from Synth (Diadema, SP, Brazil). Chloroform, dimethyl sulfoxide (DMSO), and methanol were purchased from JT Baker (Center Valley, PA, USA), and methyl *tert*-butyl ether was obtained from Vetec (Duque de Caxias, RJ, Brazil). Stock solutions of B[*a*]P at 98.0 mg L^{-1} were prepared in acetonitrile. From these solutions, diluted solutions (98.0 µg L^{-1}) were obtained in appropriate volumes. All solutions were stored in amber vials at 4 °C in the dark. The solutions were stable for over a year.

Apparatus and software

An analytical balance Shimadzu ATX 224 (Tokyo, Japan), a Velp Scientifica ZX Class vortex (Usmate, Italy), and a Corning PC420D hot plate (Corning, USA) were the support equipment used. A Agilent Varian Cary-Eclipse fluorescence spectrophotometer (Mulgrave, Australia) equipped with a xenon flash lamp was used to obtain the excitation-emission fluorescent measurements. Quartz cells with a 1.00 cm path length were used. The spectra were saved in ASCII format and transferred to a computer for subsequent manipulation.

Procedure

Test set samples

For the development and testing the applicability of the proposed method, one brand of extra virgin olive oil was purchased in a local supermarket and analyzed. The olive oil was of Portuguese origin, and according to the manufacturer, it was an extra virgin olive oil with an acidity ≤ 0.5% and peroxide ≤ 20 mEq kg^{-1}. The samples did not contain B[*a*]P or its concentration was lower than the limit of detection of the method. Thus, the samples were spiked with the analyte before the sample preparation procedure described below.

Low temperature liquid-liquid extraction

A 3.0 mL aliquot of olive oil was accurately transferred into a 15 mL glass tube. The sample was spiked and then homogenized. After, 6 mL of a solution of acetonitrile and acetone (3:2 v/v) was added and agitated by vortex at 1500 rpm for 5 min. To initiate the separation phase process, the mixture was kept at rest for 10 min before the cooling process at −18 °C for 2 h. After this time of cooling, the oil phase was completely frozen. The unfrozen top layer composed mainly of acetonitrile and acetone was easily transferred to a 50 mL beaker, and the solvent was evaporated to dryness by heating at 45 °C with a hot plate. The residue was dissolved in 2.5 mL of DMSO. Using a Pasteur pipette, the whole volume was placed into a quartz cuvette for fluorescence analysis.

Fluorescence analysis

For conventional fluorescence analysis, the emission spectra were collected in the range of 300-600 nm at a scanning rate of 600 nm min^{-1} and an excitation wavelength of 298 nm. For constant energy synchronous fluorescence, the excitation spectra were obtained by Δλ = 19 nm. The temperature was set to 20 °C. The excitation and emission slit widths were 10 and 5 nm, respectively. The solvent, temperature, slit widths, and quenching were studied as parameters to be optimized. The inner filter effect was evaluated following optimization of the extraction process. Absorption spectra were measured using a BFRL Rayleigh VIS-723G (Beijing, China) recording spectrophotometer equipped with a quartz cuvette of 1.0 cm pathlength. The maximum absorption observed was below 0.0162 AU (average of 0.012 AU). Based on these findings, the impact of the filter effect was considered negligible and subsequently disregarded.

Figures of merit

Some method performance requirements were determined (linearity, selectivity, precision, recovery, limit of quantification (LOQ), and limit of detection (LOD)) following the guidance of Instituto Nacional de Metrologia, Qualidade e Tecnologia (INMETRO).[31] These parameters were studied using standard solutions, blank, and spiked blank samples.

Linearity

Linearity was evaluated by the ordinary least squares method. A matrix matched calibration curve was constructed at six levels of B[*a*]P: 0.8, 1.4, 2.0, 2.6, 3.2, and 3.8 μg L^{-1}. The samples were analyzed randomly, and the regression parameters were estimated. The statistical methodology applied consisted of the Ryan-Joiner test of normality distribution, the Jackknife test of standardized residuals, the Durbin-Watson test of independence, and the Brown-Forsythe test of homoscedasticity. *F*-tests were employed for significance of regression and adjustment of linearity. For all tests, the significance level was 0.05.

Selectivity and matrix effect

For selectivity analysis, blank samples were analyzed to check for interferences from matrices. A solvent curve was created, following the same statistical methodology as the linearity calibration, to assess the matrix effect. The comparison of slopes between the two curves was conducted, and *F*- and *t*-tests were applied.

Recovery and precision

Trueness was assessed by means of recovery because the certified reference material was not available. Three concentration levels were studied (0.8, 2.0, and 3.2 μg L^{-1}) in six independent replicates. The acceptable range was defined as 40-120%. Precision was evaluated through relative standard deviations (RSD) of the spiked samples from the recovery experiment under repeatability (same day) and intermediate precision (different days). The criteria for acceptance were RSD lower than 30% for repeatability and lower than 45% for intermediate precision.[31]

LOD and LOQ

The LOD and the LOQ were evaluated by analysis of matrix-matched samples without the addition of B[*a*]P (blank samples) in ten independent replicates (n = 10). The LOD and LOQ were calculated as the standard deviation from the analytical signals (s_0) converted to concentration divided by the number of replicates (n) observations when the method is applied in routine analysis (n = 3) and multiplied by three (LOD = 3 signal/noise) and ten (LOQ = 10 signal/noise).

$$LOD = 3\frac{s_0}{\sqrt{n}}; \quad LOQ = 10\frac{s_0}{\sqrt{n}} \qquad (1)$$

Results and Discussion

Fluorescence analysis optimization

Effect of the solvent

The emission spectra of the B[*a*]P solutions (98.0 μg L^{-1}) were obtained in 9 different solvents to investigate their influence on the fluorescence intensity of the analyte. The standard solutions were analyzed in three independent replicates (n = 3), and the signals of the blank samples were duly subtracted. DMSO generated the highest quantum yield, as already described in the literature.[32] The high intensity observed can be attributed to the high solubility that B[*a*]P shows in this solvent.[20] It was noted that some of the solvents producing the most intense signals are the ones with the largest dielectric constant (Figure 1). It is also important to emphasize that acetone completely quenched the analyte fluorescence. As it was used for the extraction step, its impact was further evaluated. The shifts observed at λ$_{max}$ related to hypsochromic and bathochromic effects were not very significant and fluctuated from 403 nm for hexane to 407 nm for DMSO.
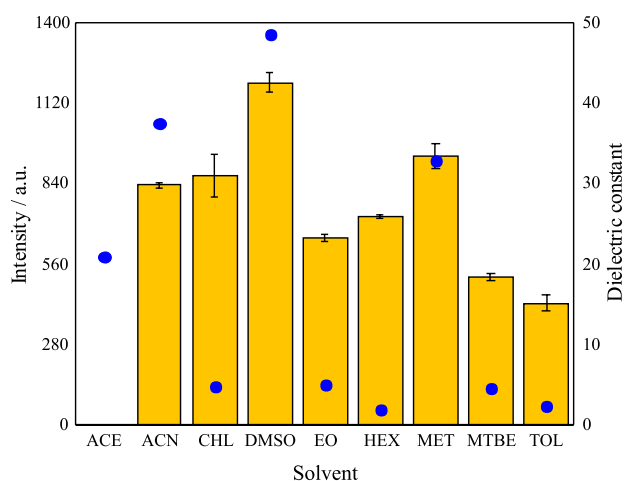

Figure 1. Average analytical signal of the fluorescence emission intensity (yellow bars) obtained for B[*a*]P (98.0 μg L^{-1}) in nine different solvents (n = 3) and their dielectric constants (blue dots). ACE: acetone; ACN: acetonitrile; CHL: chloroform; DMSO: dimethyl sulfoxide; EO: ethyl octanoate; HEX: hexane; MET: methanol; MTBE: methyl *tert*-butyl ether; TOL: toluene.

Effect of temperature

Temperature plays a crucial role in influencing both the viscosity of the solvent and the internal conversion rate of the analyte. When in the excited state, a portion of the electronic energy of the fluorophore is converted into vibrational energy. This process is facilitated by thermal stimulation, where an increase in temperature lead to a decrease in fluorescence intensity. The relationship between these factors and the fluorescence quantum yield (ϕ) is expressed by the Forster-Höffmann equation:

$$\log \phi = C + x \log \eta \qquad (2)$$

where η is the viscosity, C is a specific constant for the fluorophore, and x is a temperature dependent constant.[33] The emission spectra of the 98.0 μg L^{-1} B[*a*]P solutions were obtained in DMSO at 20, 25, and 30 °C with three independent replicates (n = 3). As expected, a significant reduction in fluorescence was observed as the temperature increased (result not shown). Because the freezing point of DMSO is 19 °C, it was not feasible to lower the temperature of the medium below 20 °C.

Effect of the quenching effect by acetone

Considering the high quenching effect of acetone on the fluorescence signal intensity of B[*a*]P (as observed in the results presented in Figure 1), it became essential to determine the maximum allowable residual concentration of acetone. To investigate this, fluorescence spectra were recorded at 20 °C for DMSO samples spiked with varying concentrations of acetone (1.000, 0.500, 0.250, 0.125, and 0.000% acetone) and containing 6.0 μg L^{-1} of B[*a*]P (Figure 2).

It is expected that there was a remaining amount of acetone in the extract, so it was verified if even a low amount of this solvent as a residue disables the detection of the analyte. The graph in Figure 2 describes the quenching effect of acetone at a residual level in the fluorescence emission.
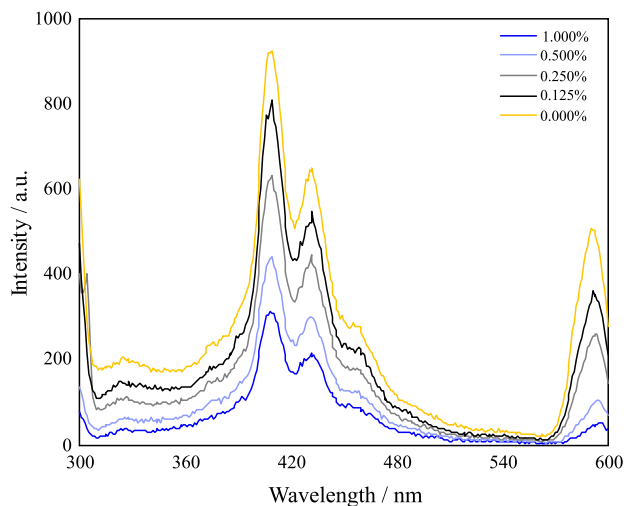

Figure 2. Typical B[*a*]P emission spectra (6 μg L^{-1}) in DMSO at different concentrations of acetone (%, v/v) at λ$_{exc}$ = 298 nm (n = 3).

4 of 8

J. Braz. Chem. Soc. **2024**, 35, 6, e-20230200

The lowest value of acetone in the sample already quenches the signal. As the percentage of acetone in the extract increased, it was observed that the quantum yield decreased drastically, which could hinder the analysis if the method was not sensitive enough. The Stern-Volmer equation describes the capacity of a quenching agent to suppress the efficiency of fluorescence emission:[34]

$$F_0/F = 1 + K_q \tau_0 [Q] \tag{3}$$

where F_0 and F are the relative fluorescence intensities of the analyte in the absence and presence of a quenching agent, respectively, K_q is the deactivation reaction rate constant, τ_0 is the half-life period of the fluorophore, and Q is the suppressor concentration. Although the quenching effect of acetone on 3-methyl-7-hydroxycoumarin is reported in the literature,[35] no publications were found demonstrating this effect in B[a]P, as PAHs are mostly affected by dissolved oxygen, nitromethane, and nitro compounds.[34] After this study, special attention was paid during the evaporation step to remove as much of the acetone as possible.

Effect of the slit width

The fluorescence signal is also defined by the amount of light that passes through the excitation (Exc) and emission (Em) monochromators. The intensity is proportional to the square of the product of both slit widths. Normally, narrower slits increase the selectivity and reduce the sensibility and *vice versa*. Until this stage, the standard values of 5 nm for excitation and 5 nm for emission were used. Extract samples containing 20 µg kg^{-1} B[a]P were analyzed using certain combinations of slits: C1 (Exc: 5.0 nm; Em: 5.0 nm), C2 (Exc: 5.0 nm; Em: 10.0 nm), C3 (Exc: 10.0 nm; Em: 5.0 nm), C4 (Exc: 10.0 nm; Em: 10.0 nm). Figure 3 shows how this parameter alters the detection of B[a]P in the matrix.

When any slit was set to 2.5 nm, the signal was extremely low, making the analysis unfit. Spectra generated at 20.0 nm were not considered either because the two characteristic peaks merge and it is not possible to assign plausible values to the intensity. Setting both slits at 5.0 nm generates a weak fluorescence that could be compromised when analyzing B[a]P at lower concentrations and due to the loss through sample preparation. Finally, having only one of the slits adjusted at 10.0 nm results in a satisfactory intensity. Despite the similarities between the combinations C2 and C3, the condition C3 was chosen because it produces less background signals.

Constant energy synchronous fluorescence (CESF)
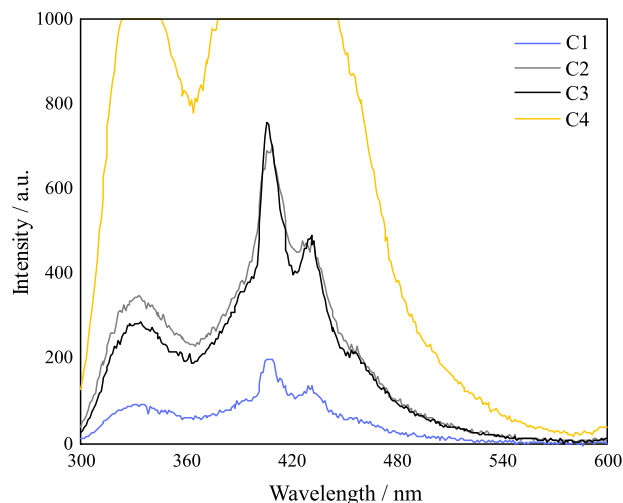
The use of CESF allowed an improvement in the

Figure 3. B[a]P emission spectra (20 µg kg^{-1}) in DMSO for different combinations of slits. C1 (Exc: 5.0 nm, Em: 5.0 nm), C2 (Exc: 5.0 nm, Em: 10.0 nm), C3 (Exc: 10.0 nm, Em: 5.0 nm), C4 (Exc: 10.0 nm, Em: 10.0 nm).

detection of B[a]P compared to conventional analysis. CESF shows the excitation spectrum. A highly defined peak at 388 nm related to B[a]P is clearly observed (Figure 4).
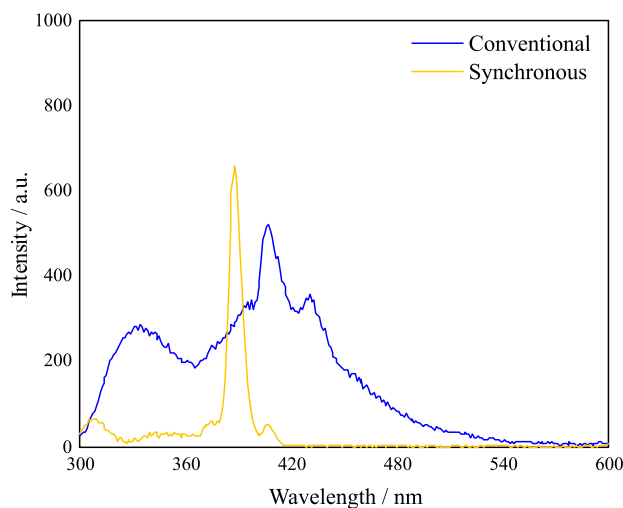

Figure 4. Comparison between conventional fluorescence (emission spectrum) and CESF (excitation spectrum) of 10 µg kg^{-1} B[a]P in matrix-matched samples.

This wavelength was used instead of the previous 298 nm because it has fewer spectral overlaps, which increases the selectivity, as noted by the more defined peak and the reduction of matrix interferences. It is also relevant to claim that CESF offers a higher intensity than common photoluminescence scanning under the same conditions.

Efficiency of the extraction

The efficiency yield was established as the ratio of the intensity of B[a]P fluorescence in the sample spiked before

J. Braz. Chem. Soc. **2024**, *35*, 6, e-20230200

5 of 8

the extraction to the intensity when the sample was spiked in the resuspended extract. Therefore, the mass of the analyte that is recovered in the procedure is 39.6% (± 0.6). This rate should not prevent the method from being a sensitive technique to determine B[*a*]P in the target level because the yield is highly reproducible under specified extraction conditions.

Figures of merit

The method suitability was checked with some figures of merit proposed by INMETRO (Table 1). For linearity determination, a Jackknife test was applied to remove outliers. Through Ryan-Joiner ($p > 10$), Brown-Forsythe ($p > 0.05$), and Durbin-Watson ($p > 0.10$) tests, all requirements were satisfied (residues followed the normal distribution, showed homoscedasticity and absence of autocorrelation, respectively). The analytical curve was linear in the studied working range (0.8-3.8 µg kg^{-1}), and the parameters estimated by the ordinary least squares method were appropriate (Table 1).

Then, the analysis of variance test (ANOVA) confirmed that the regression was significant ($p > 0.05$) and there was no deviation from linearity ($p > 0.05$). The linear range obtained includes the concentration of interest (2 µg kg^{-1}), and the method reaches the intended purpose (Figure 5).

The evaluation of the selectivity was initially consolidated via the analysis of blank samples. The analytical signal due to the olive oil extract in DMSO is much less significative when operating with CESF.

Through the calibration curve of B[*a*]P in the solvent, all the requirements for linearity were attended. Thus, the slopes of the solvent and matrix-matched calibration curves were visually similar, and by the *F*- and *t*-tests, they were compared and were exempt of the matrix effect ($p > 0.05$).

The experimental LOD and LOQ values of 0.04 and 0.15 µg kg^{-1}, respectively, were obtained.
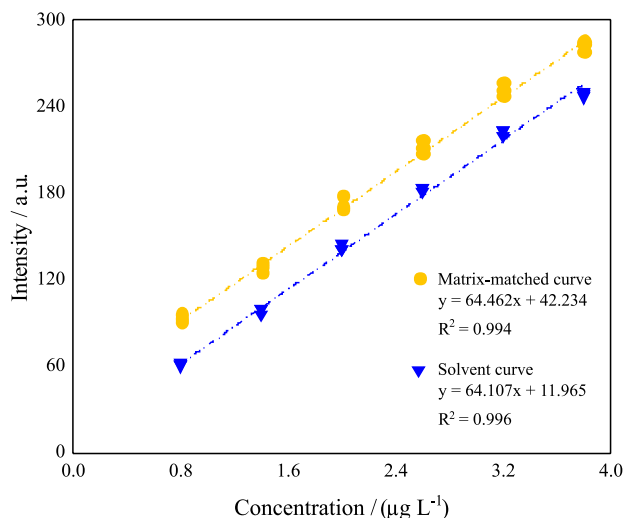

Figure 5. Comparison of the solvent and matrix-matched calibration curves of B[*a*]P for evaluation of the matrix effect (n = 3).

However, LOQ is considered the first level of the analytical curve (0.80 µg kg^{-1}) because the calculated value is below the linear range. These results are consistent to the state-of-the-art data, being better than those reported in the literature,[18,19,21,23] attesting to the potential of LTLLE CESF, mostly due to the high sensitivity of the method.

The evaluation of trueness was made through the mean recovery of spiked samples at 0.8, 2.0, and 3.2 µg kg^{-1}. Quantification of the recovery in the concentration levels was 103.1-112.0%. These results are acceptable according to the limits established by validation guide for the concentration of 1 ppb.[36] Repeatability and intermediate were 3.9-6.7 and 4.6-7.5%, respectively. Intraday and interday precision also met the requirements of the INMETRO for the concentration of 1 ppb. This method presents adequate recovery and precision for all concentration levels.

The validation results confirmed the reliability of the method developed for the determination of B[*a*]P in olive

Table 1. Figures of merit for B[*a*]P determination by the LTLLE FSEC method

B[*a*]P concentration / (µg kg^{-1})	Intraday precision		Interday precision		Mean recovery	
	RSD / %	Limit / %	RSD / %	Limit / %	Recovery / %	Limit / %
0.8	6.7	30	7.5	45	112.0	40-120
2.0	6.1	30	6.2	45	103.8	40-120
3.2	3.9	30	4.6	45	103.1	40-120
Linear range / (µg kg^{-1})	0.8-3.8					
Regression function	Slope	Intercept	Linearity (R^2)			
	64.462	42.234	0.994			
LOD / (µg kg^{-1})	0.04					
LOQ / (µg kg^{-1})	0.80					

B[*a*]P: Benzo[*a*]pyrene; LOD: limit of detection; LOQ: limit of quantification; RSD: relative standard deviation.

6 of 8

J. Braz. Chem. Soc. **2024**, 35, 6, e-20230200

Table 2. Comparison between the reference method and the proposed one

Parameter	ISO 15753[27]	Proposed method
Number of liquid-liquid extractions	3	1
Solvent volume *per* sample / mL	165	8.5
Cleanup method	solid phase extraction-C18 solid phase extraction-fluorisil	cooling at −18 °C
Solvent	acetone, acetonitrile, dicloromethane, hexane, methanol, tetrahydrofurane and toluene	acetone, acetonitrile and dimethyl sulfoxide
time	3 days	4 h
Equipment required	gas chromatography-mass spectrometry	spectrofluorometer

oil samples, attending the range of low levels that are recognized as the safety limits (2.0 µg kg⁻¹). The presented method offers a high sample throughput and reduces the time and amount of organic solvent required compared to the ISO 15753 standardized method (Table 2).[27] Importantly, the LTLLE CESF technique stands out for its simplicity and efficiency, reducing the need for chromatography and solid-phase extraction steps. However, it is noteworthy that the method's selectivity and performance can be enhanced for broader applicability, either by integrating it with chemometric tools or through the utilization of separation techniques such as chromatography or electrophoresis, to enable the detection and quantification of other PAHs or the analysis of various edible oils.

Conclusions

A liquid-liquid extraction method, originally proposed in ISO 15753:2016, was further developed by incorporating a low-temperature cleanup step and subsequent direct analysis using synchronized fluorescence at constant energy. This combined approach proved to be well-suited for the determination of B[*a*]P in olive oil. During method development, several parameters affecting fluorescence analysis were investigated, including the detection solvent, slit width, temperature, acetone quenching, and synchronous mode. The obtained results were consistent with the established literature regarding these parameters. Following the assessment of key performance indicators, the method demonstrated selectivity, accuracy, linearity, precision, and acceptable limits of quantification and detection, thus establishing its suitability for sample preparation and fluorescence analysis. Its simplicity of execution makes it an advantageous alternative for routine analyses that require high analytical frequency. Fluorescence spectroscopy, being compatible with food matrices, exhibits remarkable sensitivity and the ability to effectively discriminate the analyte in the presence of matrix interference.

Acknowledgments

Author Contributions

Willian Miguel Soares was responsible for project investigation, data curation, formal analysis, writing the original draft, review, editing and visualization; Ricardo Mathias Orlando for took in charge of the conceptualization, resources, project administration, funding acquisition, review, editing and supervision; Helvécio Costa Menezes helped with resources, project administration, review, editing and supervision.

References

1. Sienra, M. R.; Rosazza, N. G.; Préndez, M.; *Atmos. Res.* **2005**, *4*, 267. [Crossref]

2. Keith, L. H.; *Polycyclic Aromat. Compd.* **2014**, *35*, 147. [Crossref]

3. International Agency or Research on Cancer (IARC); *Monographs on the Evaluation of Carcinogenic Hazards to Humans*, vol. 92; IARC: Lyon, 2010. [Link] accessed in December 2023

4. Baird, W. M.; Hooven, L. A.; Mahadevan, B.; *Environ. Mol. Mutagen.* **2005**, *45*, 106. [Crossref]

5. Ramesha, A.; Harris, K. J.; Archibong, A. E.; *Reproductive and Developmental Toxicology*, 3rd ed.; Academic Press: Kentucky, USA, 2022. [Crossref]

6. Ni, Y.; Wang, P.; Song, H.; Lin, X.; Kokot, S.; *Anal. Chim. Acta* **2014**, *821*, 34. [Crossref]

7. Zhan, S.; Zhang, X.; Cao, S.; Huang, J.; *Fertil. Steril.* **2015**, *103*, 815. [Crossref]

8. Sun, Y.; Wu, S.; Gong, G.; *Trends Food Sci. Technol.* **2019**, *83*, 86. [Crossref]

J. Braz. Chem. Soc. **2024**, *35*, 6, e-20230200

7 of 8

9. Peng, P. L.; Lim, L. H.; *Food Anal. Methods* **2022**, *15*, 1042. [Crossref]

10. Sánchez-Arévalo, C. M.; Olmo-García, L.; Fernández-Sánchez, J. F.; CarrascoPancorbo, A.; *Compr. Rev. Food Sci. Food Saf.* **2020**, *19*, 3528. [Crossref]

11. Rose, M.; *Olives Olive Oil Health Dis. Prev.* **2010**, 637. [Crossref]

12. Mafra, I.; Amaral, J. S.; Oliveira, M. B.; *Olives Olive Oil Health Dis. Prev.* **2010**, 489. [Crossref]

13. Rodríguez-Acuña, R.; Pérez-Camino, M. C.; Cert, A.; Moreda, W.; *Food Addit. Contam.: Part A* **2007**, *25*, 115. [Crossref]

14. Commission of the European Communities; *208/2005/EC: Commission Decision of 4 February 2005*; Official Journal of the European Union, 2005, L 34, p. 3. [Link] accessed in December 2023

15. Boskou, D.; *Olive Oil: Chemistry and Technology*, 2nd ed.; AOCS Publishing: Thessaloniki, Greece, 2006.

16. Plaza-Bolaños, P.; Frenich, A. G.; Vidal, J. L.; *J. Chromatogr. A* **2010**, *41*, 6303. [Crossref]

17. Rivera-Figueroa, A. M.; Ramazan, K. A.; Finlayson-Pitts, B. J.; *J. Chem. Educ.* **2004**, *81*, 242. [Crossref]

18. Li, N.; Luo, H. D.; Jia, Y. Z.; Zhou, N.; Li, Y. Q.; *Food Addit. Contam.: Part A* **2011**, *28*, 235. [Crossref]

19. Zhou, N.; Luo, H. D.; Li, N.; Jia, Y. Z.; Li, Y. Q.; *Luminescence* **2011**, *26*, 35. [Crossref]

20. Lin, L. R.; Luo, H. D.; Li, X. Y.; Li, N.; Zhou, N.; Jia, Y. Z.; *Food Addit. Contam.: Part A* **2014**, *31*, 1219. [Crossref]

21. Cañas, A.; Richter, P.; Escandar, G. M.; *Anal. Chim. Acta* **2014**, *852*, 105. [Crossref]

22. Pena, E. A.; Ridley, L. M.; Murphy, W. R.; Sowa, J. R.; Bentivegna, C. S.; *Environ. Toxicol. Chem.* **2015**, *34*, 1946. [Crossref]

23. Liu, Y.-H.; Wu, P.-P.; Liu, Q.; Luo, H.-D.; Cao, S.-H.; Lin, G.-C.; *Food Anal. Methods* **2016**, *9*, 3209. [Crossref]

24. Cheng, W.; Liu, G.; Wang, X.; Liu, X.; Liu, B.; *J. Am. Oil Chem. Soc.* **2015**, *92*, 1725. [Crossref]

25. Kumar, K.; *J. Fluoresc.* **2020**, *30*, 613. [Crossref]

26. Li, Y.-Q.; Li, X.-Y.; Shindi, A.-A.; Zou, Z.-X.; Liu, Q.; Lin, L. R. In *Reviews in Fluorescence 2010*; Geddes, C. D., ed.; Springer: New York, 2014, p. 95.

27. ISO 15753: *Animal and Vegetable Fats and Oils: Determination of Polycyclic Aromatic Hydrocarbons*; ISO: Geneva, 2016. [Link] accessed in December 2023

28. Huang, J.-X.; Lu, D.-H.; Wan, K.; Wang, F.-H.; *Chinese Chem. Lett.* **2014**, *25*, 635. [Crossref]

29. Bertoz, B.; Pucaro, P.; Conchione, C.; Moret, S.; *Foods* **2021**, *10*, 324. [Crossref]

30. Mo, R.; Zhang, Y.; Ni, Z.; Tang, F.; *Food Sci. Biotechnol.* **2017**, *26*, 15. [Crossref]

31. Instituto Nacional de Metrologia, Qualidade e Tecnologia (INMETRO); *DOQ CGCRE-008: Orientação sobre Validação de Métodos Analíticos, Documento de Caráter Orientativo, Revisão 05-Agosto 2016*; INMETRO, 2020. [Link] accessed in December 2023

32. Falcón, M.; González Amigo, S.; Lage Yusty, M. A.; Laffon Lage, B.; Simal Lozano, J.; *Talanta* **1999**, *48*, 377. [Crossref]

33. Faust, S.; Tea, G.; Dreier, T.; Schulz, C.; *Appl. Phys. B* **2012**, *110*, 81. [Crossref]

34. Lakowicz, J. R. In *Principles of Fluorescence Spectroscopy*, 3rd ed.; Springer: New York, NY, 2008. [Crossref]

35. Sharma, V. K.; Mohan, D.; Sahare, P. D.; *Spectrochim. Acta, Part A* **2007**, *66*, 111. [Crossref]

36. Association of Official Analytical Chemists (AOAC); *Guidelines for Standard Method Performance Requirements Appendix F*; AOAC: Rockville, 2016. [Link] accessed in December 2023